CIMAC CONGRESS 25
ZURICH, MAY 19 – 23, 2025

2025 | 061

Predictive Dual-Fuel Combustion and Emission Modeling for Large Engines Using GT-Power Analysis

Simulation Technologies, Digital Twins and Complex System Simulation

Shiyan Li, Shanghai Jiao Tong University

Xinran Wang, Shanghai Jiao Tong University
Tie Li, Shanghai Jiao Tong University
Run Chen, Shanghai Jiao Tong University
Shuai Huang, Shanghai Jiao Tong University
Yibin Lv, Dalian COSCO Shipping Heavy Industry Co., Ltd
Honghua Rao, Dalian COSCO Shipping Heavy Industry Co., Ltd.
Yanzhao Liu, Dalian CRRC Diesel Engine Co., Ltd.
Xiaodong Lv, Dalian CRRC Diesel Engine Co., Ltd.

ABSTRACT

This paper presents a study on predictive dual-fuel combustion and emission modeling for large engines using GT-Power, with a focus on similarity analysis to provide accurate predictions across different engine configurations. The laminar flame speed variables were calibrated using recent spherical flame propagation speed results under elevated ambient pressure conditions, ensuring the combustion model’s accuracy. Further calibration of the Dual-Fuel model was performed using data from the SJTU-95DF and 175DF engines, as well as a V12 dual-fuel engine, covering bore sizes from 95mm to 240mm.

By integrating physics-based calibration workflows and parametric optimization of critical combustion submodels, the developed framework effectively reproduces heat release rate profiles and cylinder pressure traces. It predicts indicated thermal efficiency, exhaust gas temperature, and NHâ‚ƒ emissions within 5.0% error across diverse engine configurations. Additionally, the model distinguished two distinct regimes as AER surpasses 40% and provides a detailed energy balance breakdown. Notably, combined exhaust and cooling losses remain nearly constant across all AER conditions due to counteracting effects. As AER increases, the unburned NHâ‚ƒ ratio stabilizes around 10%, leading to a linear rise in unburned losses and a reduction in brake output power.

These findings demonstrate that the developed numerical model can be applied to various engine configurations and calibration strategies. Its accuracy in predicting key combustion parameters and ammonia emissions makes it a valuable tool for optimizing dual-fuel engines for reduced emissions and enhanced performance. The model underscores the critical trade-off between decarbonization potential and energy conversion efficiency in ammonia-diesel systems, offering insights into sustainable engine technologies and contributing to the reduction of greenhouse gas emissions in the transportation sector.

1 INTRODUCTION

The global imperative to achieve carbon neutrality has propelled dual-fuel engine technology as a critical pathway for net-zero emissions, enabled by partial displacement of diesel with low- or zero-carbon fuels. Ammonia, distinguished by its carbon-free composition, high hydrogen density (17.8 wt%), anti-knock resistance, cost-effective synthesis, and mature storage infrastructure [1], represents a particularly promising alternative [2]. However, its adoption in internal combustion engines is hindered by inherent combustion challenges, including a high autoignition temperature (650°C) and slow laminar flame speed, which is approximately one-fifth that of conventional hydrocarbon fuels [3].

The maritime industry, aligned with the International Maritime Organization's (IMO) 2050 greenhouse gas reduction targets [4]. Ammonia-diesel dual-fuel (ADDF) engines offer an effective means of decarbonizing shipping operations. Among the various injection strategies for ADDF engines, low-pressure (LP) intake-port injection has gained attention due to its retrofit compatibility with existing engine platforms and lower operational costs, supporting fuel flexibility and optimization goals in marine propulsion systems. Moreover, Li et al. reported that compared to high pressure mode, the LP ADDF mode has a potential to achieve higher indicated thermal efficiency by reducing cooling loss [5].

Experimental investigations of ADDF engines reveal critical performance-emission trade-offs. Reiter et al. [6,7] demonstrated that ammonia energy ratios (AERs) of 40–60% maintain comparable brake power while reducing CO_2 emissions by 25–38%, albeit at the expense of elevated CO, NOx, and unburned hydrocarbon emissions. Niki et al. [8,9] quantified the dual challenges of AER escalation: a 30% increase in AER correlated with 45% higher unburned NH_3 and 22% greater NOx emissions, partially mitigated through optimized pilot injection timing. Yousefi et al. [10] identified complex emission interdependencies, where 40% AER reduced NOx by 58.8% via thermal DeNOx mechanisms but paradoxically increased greenhouse gas equivalence through N_2O formation. Our parametric studies further exposed critical thresholds: at 90% AER, brake power degrades to 34% of baseline despite a 68% reduction in CO_2-equivalent emissions, while NOx exhibits non-monotonic behavior due to competing fuel-bound and thermal formation pathways [11].

While experimental studies provide fundamental insights, their utility for system optimization is constrained by three critical limitations: (1) prohibitive costs of parametric sweeps across AER, injection timing, and load domains; (2) measurement uncertainties in dual-fuel equivalence ratios; (3) inconsistent scaling laws across engine geometries. Computational modeling emerges as an indispensable complement, enabling virtual exploration of design spaces inaccessible to physical testing.

Though three-dimensional computational fluid dynamics (3D-CFD) approaches [12,13] achieve high-fidelity predictions of in-cylinder phenomena, their deployment is hindered by extreme computational demands (>10^6 core-hours per operating point) and model configuration complexity. This study instead employs a one-dimensional GT-SUITE/GT-POWER framework, leveraging validated combustion models and Navier-Stokes-based flow solutions to achieve <5% prediction error in critical parameters (power, fuel consumption, NOx) at computational speeds 10^4 times faster than 3D-CFD.

Our methodology integrates experimental datasets from in-house ADDF prototypes (95–240 mm bore) with published low-pressure injection engine data, encompassing single- and multi-cylinder configurations. GT-POWER dual-fuel combustion model was systematically calibrated using AER sweeps (0–80%), injection timing variations (~20°CA), and load transients (0.60–1.85 MPa IMEP). By resolving ammonia-diesel combustion dynamics within this framework, the study enables accurate prediction of engine performance, fuel consumption, and NH_3 emissions while demonstrating cross-platform scalability for optimization and regulatory compliance.

This work advances the development of efficient ADDF propulsion systems by providing a robust simulation tool for real-time performance monitoring, emission control strategy development, and ammonia-based technology research.

2 RESEARCH OBJECT AND SIMULATION CONDITIONS

2.1 Research object

The primary objective of this study is to develop a suite of one-dimensional (1D) predictive models for ammonia–diesel dual-fuel (ADDF) engine systems using GT-POWER, enabling accurate prediction of performance (brake power, thermal efficiency), fuel consumption, and emissions (NH_3, NOx) across diverse engine architectures, including:

- SJTU95 engine: a turbocharged inline 4-cylinder, 95 mm bore, ADDF prototype engine, model calibration.

- SJTU175 engine: a single-cylinder research engine, 175 mm bore, marine auxiliary, model calibration.

- V240 engine: a turbocharged V12 engine, 240 mm bore, marine propulsion, model validation.

Figure 1(a) and (b) display the engine test benches for the SJTU95 and SJTU175 engines at Shanghai Jiao Tong University, and the detailed engine specifications are provided in Table 1. These engines were selected to span a broad range of operational conditions—from small to large engine sizes—and to cover common configurations used in marine and industrial applications.

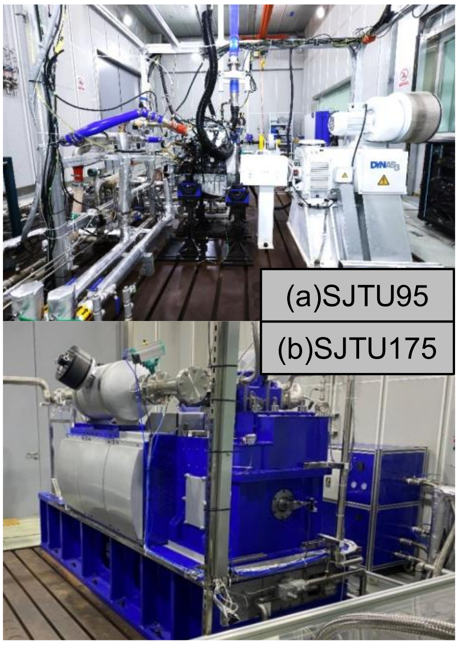

Figure 1. Ammonia-diesel dual-fuel (ADDF) engine test bench @ Shanghai Jiao Tong University.

Table 1. Specifications of ADDF engines

Parameters	SJTU95	SJTU175	V240
Cylinder number (-)	4 in-line	1	12 V-type
Bore (mm)	95	175	240
Stroke ()	102	195	275
CR (-)	17.5	15.5	14.5
IVO/IVC (°ATDC)	360/574	321/564	313/578
EVO/EVC (°ATDC)	143/360	127/392	135/408
Rated power (kW)	112 @2800rpm	215 @2100rpm	2022 @1000rpm
Fuel injection	Common rail diesel + low-pressure ammonia		
$P_{inj,\ D}$ (MPa)		120	
Rated power (kW)	112 @2800rpm	215 @2100rpm	2022 @1000rpm

2.2 Simulation conditions

In all simulations, the engine speed is fixed at 1000 rpm. The calibration process begins with the SJTU95 and SJTU175 engines, where abundant bench test data is used as the calibration reference. These models are first calibrated under pure diesel mode, across various load conditions. Subsequently, in the ammonia-diesel (ADDF) mode, additional validation is performed for the SJTU95 engine by adjusting the diesel injection timing and varying the ammonia energy ratio (AER). This calibration process ensures accurate predictions of engine behavior under different operating conditions.

For the V240 engine, data provided by the engine manufacturer is used to validate the model under a fixed load condition (IMEP = 1.85 MPa) with varying AER. This step is crucial for confirming the model's applicability across a broader range of engine configurations and operating scenarios. The simulation conditions, including all the parameters and configurations, are summarized in Table 2.

Parameters	SJTU95 (Calibration)	SJTU175 (Calibration)	V240 (Validation)
Engine speed (rpm)	1000	1000	1000
Target IMEP (MPa)			
● Diesel mode	0.60, 0.85	1.00,1.20,1.45	1.85
● ADDF mode	0.85	1.45	1.85
Inj. timing (°ATDC)	Sweep	Fixed	Fixed
AER (%)	0/20/40/60/80	0/40/80	0/35/65/80

3 SIMULATION METHODOLOGY

The computational framework integrates GT-POWER's dual-fuel combustion model to simulate engine performance, emissions, and parametric optimization (e.g., injection timing, AER, load). This framework incorporates the following fundamental assumptions:1) The working fluid is treated as an ideal gas with perfect mixing conditions within the cylinder. 2) Gas flow processes through valves and ports are modeled as quasi-steady state phenomena. 3) The intake and exhaust systems are simplified using one-dimensional flow representation, governed by the conservation laws of mass, energy, and momentum, coupled with the ideal gas equation of state. Key parameters and model components are introduced as follows.

3.1 Pre-calibrated parameter

To balance computational efficiency and extrapolation accuracy, critical parameters were prioritized: 1) Fuel injection rate: Measured using techniques such as the Bosch long-tube method, and the correlation between actual vs. electrical injection widths and delays can be obtained simultaneously. It is particularly important for simulations under high AER and short diesel pulse width conditions. 2) Intake/exhaust temperature and pressure: These are obtained from sensor measurements, and the data could be cross validated using turbocharger MAP diagrams. 3) Heat transfer and friction: The Woschini heat transfer model is used in conjunction with motoring test data to calibrate friction work.

3.2 Combustion and emission model

3.2.1 Laminar burning velocity model

Equation 1 calculates the laminar burning velocity in the dual-fuel combustion model. This model plays a crucial role in predicting the combustion characteristics of the fuel mixture under controlled conditions, particularly in terms of flame propagation and heat release in the engine.

$$S_L = \left(B_m + B_\phi(\phi - \phi_m)^2\right)\left(\frac{T_u}{T_{\mathrm{ref}}}\right)^{\alpha}\left(\frac{P}{P_{\mathrm{ref}}}\right)^{\beta} \quad (1)$$

where: S_L: Laminar flame speed, B_m: Maximum Laminar Speed, B_Φ: Laminar Speed Roll-off Value, Φ: In-cylinder equivalence ratio, Φ_m: Equiv. Ratio at Max. Speed, P: Pressure, P_{ref} = 101.3kPa, T_{ref} = 298 K, T_u: Temperature of the unburned gas, α: Temperature Exponent, and β: Pressure Exponent.

In this study, S_L is refined through most recent experimental work [14] and fitted (as shown in Equation 2) across initial temperatures (298–500K) and pressures (0.1–1MPa). Figure 3 validates predictions against experimental laminar flame speed data, ensuring more accurate and consistent combustion rate predictions in the dual-fuel framework.

$$S_L = (8.28 - 40.03 * (\phi - 1.12)^2)\left(\frac{T_u}{298}\right)^{1.7354}\left(\frac{P}{101}\right)^{-0.2638} \quad (2)$$

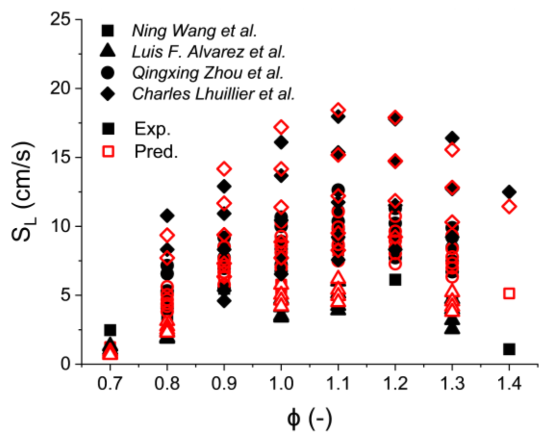

Figure 2. Comparison of experimental results and empirical correlations using Eq. 2 for laminar flame burning velocity of ammonia fuel.

3.2.2 Combustion calibration model

The dual-fuel combustion model, as implemented in GT-POWER, is adjusted by optimizing multipliers for key combustion calibration parameters—namely, the entrainment rate, ignition delay, premixed, and diffusion combustion rates. Calibration is performed against experimental heat release rate profiles as well as combustion phasing parameters (e.g., CA10, CA50, CA90).

3.2.3 Emission model

Emissions are calculated with special attention to unburned NH_3, and it is tightly coupled with the combustion model and clearance volume. Although NOx and N_2O predictions are feasible with additional calibration or reaction mechanisms, their extrapolation remains limited; hence, NOx and N_2O is not discussed further.

3.3 Model calibration Process

The calibration process is conducted in several steps: 1) Geometric setup: Defined combustion chamber dimensions and turbocharger boundary conditions. 2) Motoring Calibration: Verified friction loss, motored pressure-volume diagram and airflow characterization matched with turbocharger MAP. 3) Diesel-only calibration: Check both the heat transfer and friction coefficients, validate combustion models against cylinder pressure and power output data. 4) ADDF calibration: Parameterized key multipliers related with dual fuel model.

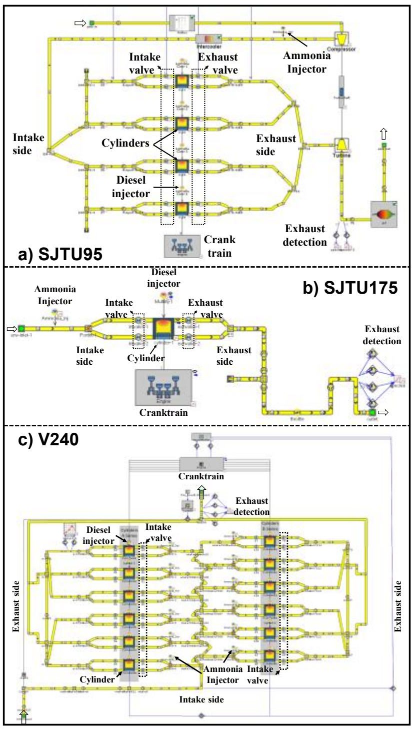

Figure 3. GT-POWER simulation models of (a) SJTU95, (b) SJTU175, and (c) V240 engine configurations.

Figure 3 illustrates the three one-dimensional engine simulation models, each comprising essential components, including intake port, ammonia injection valve, intake valve, cylinder, diesel injector, exhaust valve, exhaust port, exhaust gas measurement module, and crankshaft.

4 RESULTS

4.1 Combustion calibration of diesel model

Calibration of pure diesel combustion performance focuses on two critical aspects: the global heat transfer coefficient in the cylinder thermal submodel and key parameters in the EngCylCombDualFuel framework. These include the Entrainment Rate Multiplier (ERM), Ignition Delay Multiplier (IDM), Premixed Combustion Rate Multiplier (PCRM), and Diffusion Combustion Rate Multiplier (DCRM).

Figure 4(a) demonstrates excellent agreement between the cycle-averaged in-cylinder pressure traces (300 consecutive cycles) and simulation predictions for the SJTU95 engine at diesel model of IMEP = 0.60MPa, across various injection timings. Notably, as injection timing advances toward top dead center (TDC), IDM decreases (from 1.25 to 1.15), PCRM increases (from 0.28 to 0.70), and DCRM decreases (from 0.50 to 0.40). Similar calibration performance is observed at 75% load, with increased DCRM values indicative of intensified diffusion-dominated combustion under high-load conditions.

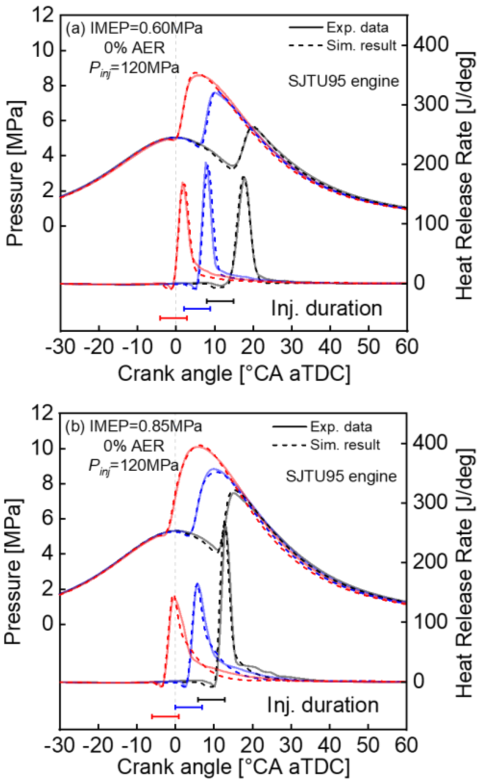

Figure 4. Comparison of cylinder pressure and heat release rate profiles for SJTU95 engine in diesel mode at IMEP of (a) 0.60 MPa and (b) 0.85 MPa.

Figure 5 presents a comparative analysis of key operational parameters including indicated thermal efficiency (η_i), global excess air ratio (λ), exhaust temperature and pressure before turbine inlet. Notably, both the global λ and exhaust temperature exhibit progressive decreases with advanced injection timing, while the exhaust pressure demonstrates minimal variation. Experimental observations reveal that the indicated thermal efficiency remains comparable across different load conditions when pilot diesel fuel injection occurs before TDC. Interestingly, even under higher load condition, no significant reduction in indicated thermal efficiency when the injection is further retarded. Furthermore, the simulation demonstrates strong agreement with experimental data, with majority of parameter predictions maintaining errors within ±3%. This validates the high accuracy of the pure diesel combustion model implementation in SJTU95 engine.

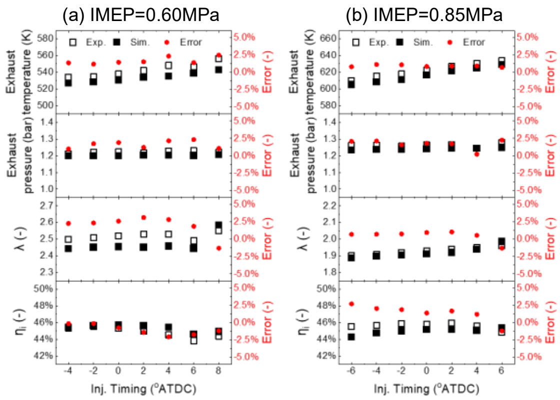

Figure 5. Comparative analysis of key operational parameters for SJTU95 engine in pure diesel mode at IMEP of (a) 0.60 MPa and (b) 0.85 MPa.

Figures 6 and 7 extend these comparisons to the SJTU175 and V240 engines at diesel operation mode, establishing a solid foundation for ADDF model calibration.

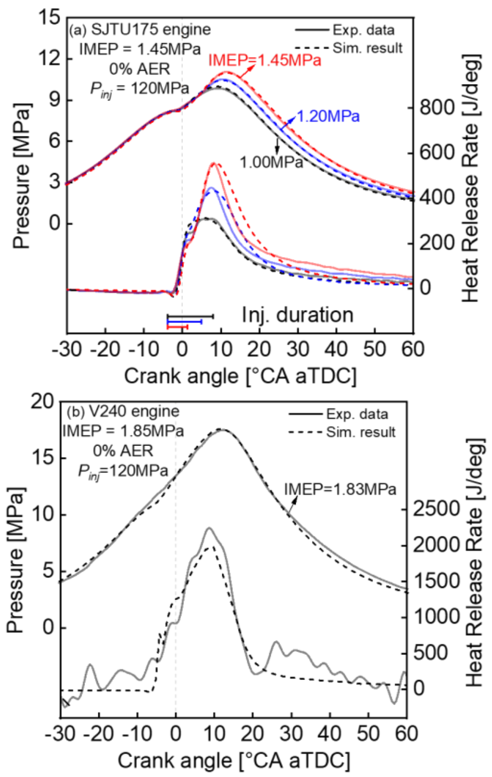

Figure 6. Cylinder pressure and heat release rate comparison for (a) SJTU175 and (b) V240 engines in pure diesel combustion mode.

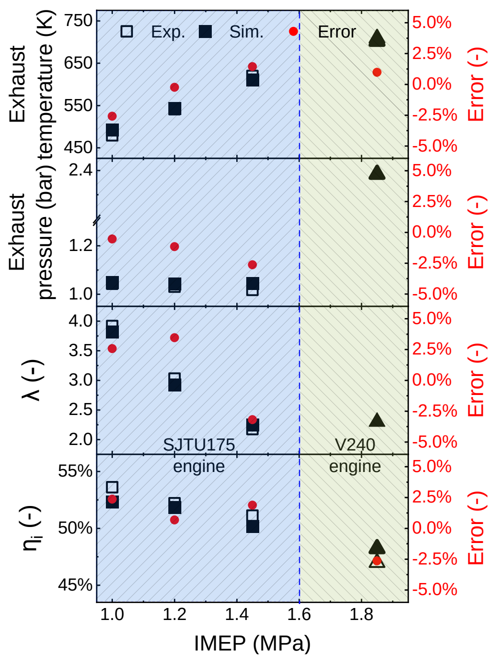

Figure 7. Operational parameter comparison for (a) SJTU175 and (b) V240 engines under pure diesel mode.

4.2 Combustion calibration and validation of ADDF model

Figure 8 compares in-cylinder pressure traces and heat release rates for the SJTU95 engine in ADDF mode at IMEP=0.85MPa and MBT (maximum brake torque) timing with varying AER conditions. As the ammonia energy fraction increases, the optimal diesel injection timing progressively advances. The heat release rate initially intensifies as ammonia energy fractions rise from 0% to 40%, but plateaus at higher fractions due to prolonged ignition delays. Corresponding calibration parameters demonstrate systematic adjustments. Further analysis reveals that between AER values of 40% and 60%, a noticeable shift occurs in combustion-related parameters. Specifically, the Entrainment rate multiplier (ERM) decreases rapidly from 3.5 to 1.0 until AER reaches 40%, after which it remains relatively stable. This rapid decrease in ERM reflects the initial transition from a highly diffusion-dominated combustion process to a more balanced combination of diffusion and premixed combustion as ammonia content increases. The Ignition delay multiplier (IDM) becomes less sensitive to changes in AER before AER reaches 40%. Concurrently, both Premixed combustion rate multiplier (PCRM) and Diffusion combustion rate multiplier (DCRM) increase significantly, reflecting an enhanced premixed and diffusion combustion phase at lower AERs as diesel fuel still dominates the combustion.

Beyond an AER of 40%, IDM begins to rise as the ignition delay increases due to ammonia's slower combustion properties, making the system increasingly reliant on diffusion combustion. At this point, ERM stabilizes, PCRM gradually decreases and DCRM increases continuously as the efficiency of "traditional" premixed combustion diminishes due to prolonged ignition delays and the increasing dominance of diffusion combustion. Furthermore, adjustment of the diffusion combustion rate control model is necessary when the AER reaches 80% to meet the final diffusion intensity inside the engine.

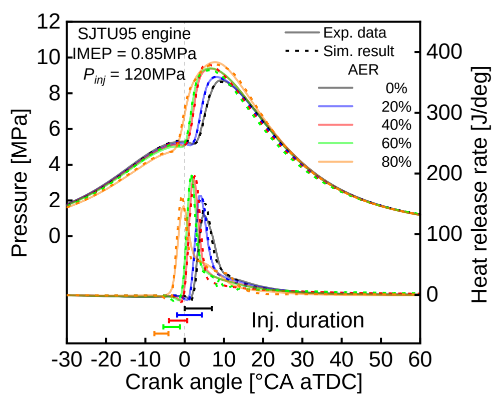

Figure 8. Cylinder pressure and heat release characteristics of SJTU95 engine in ADDF mode at IMEP=0.85 MPa across varying AER conditions.

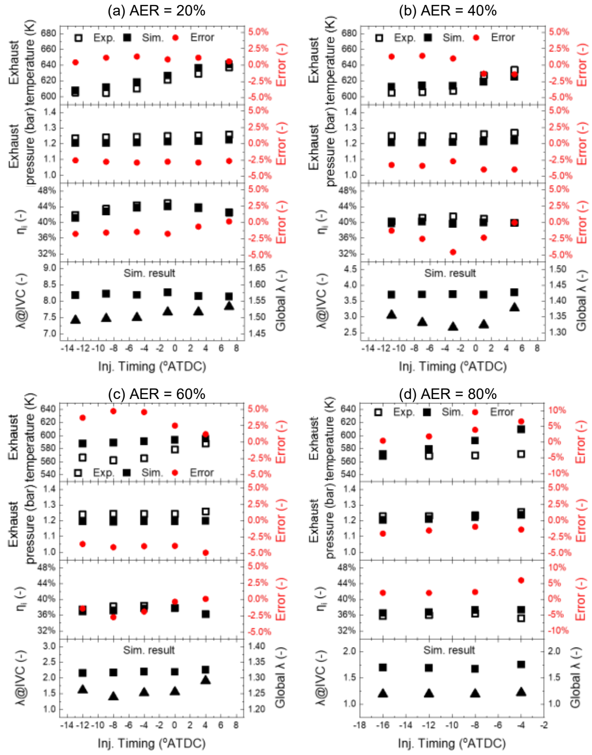

Figure 9. Operational parameter trends for SJTU95 engine in ammonia-diesel mode at IMEP 0.85 MPa with increasing AER.

Figure 9 shows trends in engine operational parameters as AER increases at IMEP=0.85MPa condition. While the exhaust temperature remains stable up to 40% AER, a rapid reduction occurs at higher substitution levels at same injection timing. Due to measurement inaccuracies in dual-fuel equivalence ratios from the MEXA-one system, critical parameters are redefined: the ammonia-specific excess air ratio at intake valve closing (IVC) exceeds 2.0 even at 60% AER condition, while the global excess air ratio reflects the total fuel mixture. These metrics confirm weak flame self-propagation in ammonia-diesel combustion, necessitating reliance on diesel spray entrainment for sustained combustion.

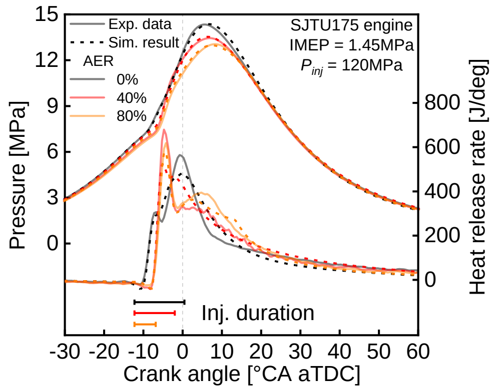

Figure 10. Combustion characteristics comparison for SJTU175 engine in ammonia-diesel mode at IMEP of 1.45 MPa under different ammonia energy fractions

Figure 10 depicts in-cylinder pressure traces and heat release rates for the SJTU175 engine in ADDF mode at IMEP=1.45MPa with varying AERs. It can be observed that as AER increases, the overall trend is similar to the results shown for the SJTU95 engine. However, due to the constant injection timing, the ignition delay increases, necessitating an increase in IDM. The changes in other parameters can be constrained by the variation trends from the previous calibration results, further verifying a quick and accurate prediction model for ADDF engine.

Finally, using the aforementioned model validation approach, the in-cylinder combustion of the V240 engine under varying AER conditions was successfully predicted. Despite limited data and significant measurement variability, the developed ADDF model demonstrated robust predictive capability for ammonia-diesel combustion modes, achieving sufficient accuracy (±8% error in peak pressure predictions) to meet system-level simulation requirements for marine engine optimization.

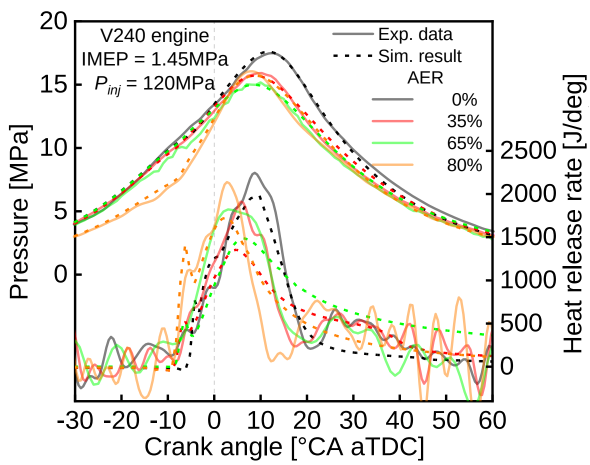

Figure 11. Cylinder pressure and heat release analysis for V240 engine in ADDF mode at IMEP 1.85 MPa with progressive ammonia substitution.

4.3 Discussion of NH_3 emission

Accurate prediction of unburned ammonia emissions relies heavily on the precise calibration of the laminar flame speed model within the combustion framework. Once combustion characteristics are well calibrated, the prediction error for unburned ammonia remains within approximately 5%. In this study, high unburned ammonia levels were observed—exceeding 10,000 ppm for the SJTU95 engine at 60% AER and 20,000 ppm for the SJTU175 and V240 engines at 80% AER. Conversion of these values to the unburned NH_3 ratio (unburned NH_3/input NH_3) shows a baseline ratio of approximately 10.0%, with the pilot injection timing ranging from -13°CA to 7°CA ATDC. Notably, under post-TDC injection conditions, flame propagation tends to stagnate, especially at higher ammonia substitution levels, where unburned NH_3 accumulates in piston crevices and flame-free zones, resulting a rapid increase of unburned NH_3 ratio. For V240 engine, a higher unburned NH_3 ratio compared to the previous baseline is observed. However, due to the lack of ammonia emission data under other operating conditions, the actual trend of unburned NH_3 ratio cannot be confirmed.

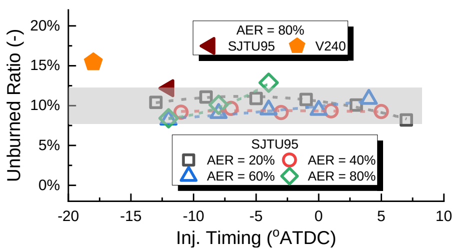

Figure 12. Comparison of unburned ammonia ratios across three engines at different AERs.

4.4 Energy balance of ADDF engine

Figure 13 illustrates the energy balance diagrams for the three engine configurations under different AER conditions. For the SJTU95 engine, as MBT timing advances with increased AER, cooling losses increase by approximately 7%, while exhaust losses decrease due to lower combustion temperatures, keeping the total thermal losses around 56%. For the SJTU175 and V240 engines—where pilot injection timing is fixed—both exhaust and cooling losses show minimal variation, with cumulative thermal losses stabilized around 50%. Consequently, as the AER increases, brake output decreases due to a linear rise in unburned losses.

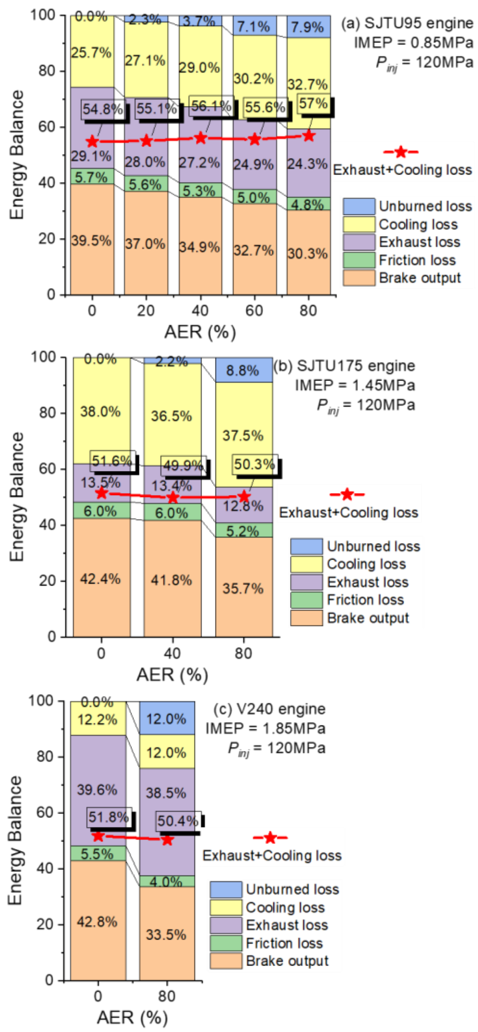

Figure 12. Energy balance diagrams for three engine configurations under varying AERs.

5 CONCLUSIONS

Based on experimental and simulation studies of low-pressure ammonia–diesel dual-fuel engines, the following key conclusions have been drawn:

- Through the optimization of submodels for heat transfer, diesel combustion, and ammonia-diesel dual fuel combustion within GT-POWER, a robust and predictive model for ammonia–diesel combustion has been successfully developed. This model demonstrates high fidelity in reproducing and in-depth analysis of engine performance and NH_3 emission characteristics across a wide operating range.

- As the ammonia energy fraction increases, the exhaust gas temperature gradually decreases. Moreover, the effect of delaying diesel injection on exhaust temperature diminishes with higher AER.

- As the ammonia energy fraction increases, the exhaust gas temperature gradually decreases. Moreover, the effect of delaying diesel injection on exhaust temperature diminishes with higher AER.
- Increased AER results in a significant rise in unburned NH_3 emissions, particularly in regions of the combustion chamber (such as piston crevices) where diesel spray and flame coverage are inadequate. This unburned ammonia is the primary factor limiting engine efficiency in low-pressure ADDF operation.

These conclusions highlight the delicate trade-offs in LP-ADDF engine operation and underscore the importance of accurate simulation models for the development of optimized combustion strategies and emission control in future ammonia-based propulsion systems.

6 DEFINITIONS, ACRONYMS, ABBREVIATIONS

ADDF: Ammonia-diesel dual-fuel

LP: Low-pressure

AER: Ammonia energy ratio

IMEP: Indicated mean effective pressure

P_{inj}: Injection pressure of diesel fuel

S_L**:** Laminar flame speed

B_m**:** Maximum Laminar Speed

B_Φ**:** Laminar Speed Roll-off Value

Φ**:** In-cylinder equivalence ratio

Φ_m**:** Equiv. Ratio at Max. Speed

P**:** Pressure

P_{ref}**:** Reference pressure (101.3kPa)

T_{ref}**:** Reference temperature (298 K)

T_u**:** Temperature of the unburned gas

α**:** Temperature Exponent

β**:** Pressure Exponent.

ERM: Entrainment Rate Multiplier

IDM: Ignition Delay Multiplier

PCRM: Premixed Combustion Rate Multiplier

DCRM: Diffusion Combustion Rate Multiplier

7 ACKNOWLEDGMENTS

This work was supported by the National Natural Science Foundation of China (Grant NO. 52306156), the Oceanic Interdisciplinary Program of Shanghai Jiao Tong University (Grant NO. SL2023MS003) and the Major International (Regional) Joint Research Project of the National Natural Science Foundation of China (Grant NO. 52020105009).

8 REFERENCES AND BIBLIOGRAPHY

[1] Wilkinson I. Siemens green Ammonia 1st NH3 European event[C]. Netherlands; Rotterdam; 2017.

[2] Laiminger S, Payrhuber K, Wermuth N, Wimmer A. The role of gas engines in a future energy market with sustainable fuels. 30th CIMAC World Congress, Korea, 2023.

[3] Woo Y, Jang J Y, Lee Y J, et al. Recent progress on the ammonia-gasoline and the ammonia-diesel dual fueled internal combustion engines in Korea[C].Proceedings of the NH3 Fuel Conference, Des Moines, IA, USA. 2014: 21-24.

[4] The 80nd session of its Marine Environment Protection Committee (MEPC 80). International Maritime Organization. July 2023.

[5] Li T, Zhou X, Wang N, Wang X, Chen R, Li S, Yi P. A comparison between low-and high-pressure injection dual-fuel modes of diesel-pilot-ignition ammonia combustion engines. Journal of the Energy Institute. 2022,102:362-73.

[6] Reiter A J, Kong S C. Combustion and emissions characteristics of CI engine using dual ammonia-diesel fuel[J]. Fuel, 2011,90:87-97.

[7] Reiter A J, Kong S C. Demonstration of compression-ignition engine combustion using ammonia in reducing greenhouse gas emissions[J]. Energy & Fuels,2008, 22(5), 2963-2971.

[8] Niki Y. Experimental Investigation of effects of split diesel-pilot injection on emissions from ammonia-diesel dual fuel engine[C]. ASME Internal Combustion Engine Division Fall Technical Conference. 2021, 85512.

[9] Niki Y, Nitta Y, Sekiguchi H, et al. Diesel fuel multiple injection effects on emission characteristics of diesel engine mixed ammonia

gas into intake air[J]. Journal of Engineering for Gas Turbines and Power, 2019,141(6).

[10] Yousefi, Amin, et al. A study on split diesel injection on thermal efficiency and emissions of an ammonia/diesel dual-fuel engine[J]. Fuel, 2022,316:123412.

[11] Wang X, Li T, Chen R, Li S, Kuang M, Lv Y, Wang Y, Rao H, Liu Y, Lv X. Exploring the GHG reduction potential of pilot diesel-ignited ammonia engines-Effects of diesel injection timing and ammonia energetic ratio. Applied Energy. 2024,357:122437.

[12] Zhou X, Li T, Wang N, Wang X, Chen R, Li S. Pilot diesel-ignited ammonia dual fuel low-speed marine engines: A comparative analysis of ammonia premixed and high-pressure spray combustion modes with CFD simulation. Renewable and Sustainable Energy Reviews. 2023,173:113108.

[13] Jin S, Wu B, Zi Z, et al. Effects of fuel injection strategy and ammonia energy ratio on combustion and emissions of ammonia-diesel dual-fuel engine[J]. Fuel,2023, 341, 127668.

[14] Wang N, Li T, Guo X, Wu Z, Huang S, Zhou X, Li S, Chen R. Laminar burning characteristics of ammonia and hydrogen blends at elevated initial pressures up to 2.5 MPa. Chemical Engineering Journal. 2024,500:157283.